Development of event-driven optimal control for central air-conditioning systems

PLEASE CITE THE PUBLISHED VERSION

https://doi.org/10.1080/19401493.2020.1737231

PUBLISHER

Taylor and Francis

VERSION

AM (Accepted Manuscript)

PUBLISHER STATEMENT

This is an Accepted Manuscript of an article published by Taylor & Francis in Journal of Building Performance Simulation on 17 Mar 2020, available online: https://doi.org/10.1080/19401493.2020.1737231

LICENCE

CC BY-NC-ND 4.0

REPOSITORY RECORD

Hou, Jin, Xiaowei Luo, Gongsheng Huang, Linfeng Zhang, Zhun Jerry Yu, and Mahroo Eftekhari. 2020. "Development of Event-driven Optimal Control for Central Air-conditioning Systems". figshare. https://hdl.handle.net/2134/11996613.v1.

Development of event-driven optimal control for central air-conditioning systems

Jin HOU[a], Xiaowei LUO[a], Gongsheng HUANG[a*], Linfeng ZHANG[a,b], Zhun (Jerry) YU[c], Mahroo EFTEKHARI[d]

[a]Department of Architecture and Civil Engineering, City University of Hong Kong, Kowloon, Hong Kong

[b]Department of Underground Engineering, Southeast University, Nanjing, Juangsu, 211189, China

[c]College of Civil Engineering, National Center for International Research Collaboration in Building Safety and Environment, Hunan University, Changsha, Hunan, 410082, China

[d]School of Architecture, Building and Civil Engineering, Loughborough University, Leicestershire, U.K.

*The corresponding author: email gongsheng.huang@cityu.edu.hk; Tel 852-34422408

Abstract

Event-driven optimal control was recently developed for central air-conditioning systems to speed up the response of optimal control to irregular changes in the system optioning conditions. In a time-driven paradigm usually the optimization is carried out with a constant frequency, however the event-driven optimal control triggers optimization actions by events, which will be essentially defined to catch up with the irregular changes. Considering that the occurrence of events should imply the necessity to execute optimization, this paper investigates the necessity of optimization actions, based on which a new method to develop event-driven optimal control law is proposed. This can naturally lead to the establishment of an event-action map. This map indicates that not all the decision variables should be optimized when an event occurs, different from other methods that require optimizing all decision variables. The merits of the new method were also demonstrated using several case studies.

Keywords: Real-time optimal control; Event-driven optimization; Energy efficiency; Air-conditioning system

1. Introduction

Real-time optimal control is an approach to optimize the operation of central air-conditioning (AC) systems and hence improve their energy efficiency without sacrificing indoor thermal comfort (Chua et al. 2011; ASHRAE 2015). It always optimizes the set-points for the local

controllers in AC systems in response to the changes in their working condition, including outside weather and indoor thermal conditions (Wang 2009). Real-time optimal control has undergone rapid developments since the 1980s (Cumali 1988). Most research have concentrated on the formulation of optimization problems (Kelman, Ma and Borrelli 2013; Wang and Ma 2008) and the development of advanced optimization techniques, such as evolutionary algorithms (Fong, Handy, and Chow 2009; Ma and Wang 2011) and branch and bound (Chang, Lin, and Lin 2009; Fisk 2014).

In the current real-time optimal control, most current strategies adopts a time-driven paradigm (Kusiak, Li, and Tang 2010; Sun et al. 2013; Martyr et al. 2019), i.e. optimization actions are triggered following a fixed frequency or a scheduled timetable during operation of AC systems. For example, Nassif (2005) developed a bi-objective optimal control strategy for an AC system, in which the supply air and the chilled water supply temperatures were optimized every 30 minutes. However, in the operation of a central AC system, many changes are stochastic and hard to predict, such as those in the weather, load, and occupancy conditions. Being a periodic mechanism in nature, time-driven optimal control (TDOC) may fail to capture those aperiodic changes and thus cannot perform the optimization at the right time (Ma, Matusko, and Borrelli 2015). It may also waste the computational resources when the operating conditions are stable, and no optimization is necessary (but is still performed).

The event-driven paradigm offers an alternative to the time-driven paradigm. Its core idea is that "an action should be triggered by an 'event' that is specified as a well-defined condition on the system state or as a random state transition" (Cassandras 2014). The event-driven approach has been used in sampling (Astrom and Bernhardsson 1999), estimation (Xia, Gupta, and Antsaklis 2016), control (Shen, Yan, and Zhang 2016; Borgers, Dolk, and Heemels 2017) and optimization (Cao 2008), and it is especially attractive when many components are connected over a shared network. For example, in the network control system, using the event-driven method can be more efficient as information transmission (the action) is triggered only when there is a significant change in the plant output measurements (the event) (Zhu, Xia, and Antsaklis 2014).

The event-driven approach has also gain primary applications in AC systems in recent years.

66 It has been used in the adaptive control of AC systems (Dhar, Verma, and Behera 2017),
67 building energy management (Xu et al. 2017), and the optimal control of the air-loop of an AC
68 system (Wu, Jia, and Guan 2015; Jia et al. 2018). In the work of Jia et al. (2018), the set-points
69 of the supply air temperature and air volumes were optimized (the action) when state variables,
70 such as the indoor air temperature, crossed the boundary of a predefined range (the event). A
71 whole central AC system including both water and air loops was considered in Wang et al.'s
72 studies, where events were defined using a knowledge-based method (Wang et al. 2016; Wang
73 et al. 2018) or a data mining approach (2017). All these studies showed that compared with the
74 TDOC, the event-driven optimal control (EDOC) was able to capture the aperiodic changes in
75 the operations of HVAC systems, and simultaneously the computational load of the EDOC can
76 be saved significantly. It should be noted that there are many factors that limit the general
77 application of optimal control for HVAC systems and computational complexity might not be
78 the critical one. However, to perform the optimization at the right time and reduce the
79 computational complexity could improve the cost-to-benefit ratio of implementing the real-
80 time optimal control in HVAC systems.
81
82 Despite these merits of EDOC, there are several limitations in these previous studies. First, the
83 knowledge-based or the data mining method are not a systematic way to define events. Try-
84 and-error should be used to access how "good" the defined events are. Second, in these studies
85 a direct map between events and individual decision variables has not been established. When
86 an event occurs, all the decision variables must be optimized. This might not be an efficient
87 method to execute optimization, especially when many variables are needed to be optimized.
88 It is possible that the occurrence of an event might only affect part of the decision variables,
89 and hence for this event only those decision variables that are affected should be optimized.
90
91 This paper proposed a study to overcome the abovementioned limitations. Considering that the
92 occurrence of events should imply the necessity to execute optimization, this paper investigates
93 the necessity of optimization actions, based on which a new method to develop event-driven
94 optimal control is proposed. This new method identifies the state transitions that have a critical
95 influence on the performance of the real-time optimal control to establish a mathematical
96 relationship between the variation in the optimal values of a decision variable and its critical
97 state transitions. According to this relationship, an EDOC law is set up and naturally, this

98   EDOC law leads to the definition of an event and action space as well as the map between them.

99   The event-action map is used to specify which decision variable should be optimized when an

100 event occurs, which indicates that that not all of the decision variables should be optimized

101 when an event occurs, which is different from a traditional strategy that requires to optimize

102 all decision variables.

103

104 Considering the mutual interactions among the decision variables, the event and action spaces

105 are improved through action and/or event merging after analyzing the interaction among the

106 decision variables. Case studies are used to demonstrate the development of the EDOC strategy

107 for a typical central AC system. The performance of the developed strategy is assessed using

108 multiple evaluation indices and compared to that of a TDOC method. It is worth noting that

109 since the proposed method is based on the optimization necessity; it is universal and not limited

110 to the application in AC systems.

111

112 This paper is organized as follows. Section 2 illustrates the necessity of optimization actions.

113 Section 3 shows the procedure to establish the event and action spaces for EDOC as well as

114 the map between them. Section 4 presents case studies, including the simulation platform for a

115 typical AC system and the development of the EDOC law. Result analysis and discussion are

116 shown in Section 5. Concluding remarks are presented in Section 6.

117

118 **2. Necessity of optimization actions**

119 Before the illustration of EDOC strategy development method for AC systems, the necessity

120 of optimization actions is firstly introduced, which lays the foundation of the proposed

121 development method. Assume there is a simple system, where only a state variable and a

122 decision variable are involved as shown in Eqn. (1) and (2). The state variable s refers to the

123 uncontrollable operation condition, and the decision variable v is controllable by resetting its

124 value.

125
$$F = f(s(t), v) \tag{1}$$

126
$$v^{opt}(t) = \arg\min_v f(s(t), v) \tag{2}$$

127 During the operation of the system, the state variable s varies in the time dimension as shown

128 in Fig. 1. Optimization actions $act_1, act_2, \cdots$ are executed in a row to minimize the objective

129 function f in real time by searching the decision variable's optimal values $v_1^{opt}, v_2^{opt}, \cdots$

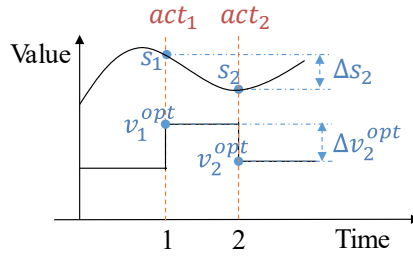130   under the state variable's instantaneous values $s_1, s_2, \cdots$.

131

132   **Fig. 1**. The state transition and variation of the decision variable's optimal value

133

134   Conceptually, an optimization action is necessary when the current value of the decision

135   variable is no longer optimal. Therefore, act_2 is necessary due to non-zero Δv_2^{opt}, the

136   variation of the searched decision variable's optimal value by act_2 from that by act_1.

137   Furthermore, the larger the deviation, the performed optimization action has the higher

138   necessity. Considering that the variation of the decision variable's optimal values is caused by

139   changes of the state variable, an event will be defined as these state variables' changes leading

140   to an obvious variation of decision variables' optimal values. Events defined in this way will

141   certainly drive optimization actions with a high necessity.

142

143   **3. Methodology**

144   The development method of EDOC strategy for AC systems consists of three steps: 1)

145   identification of critical state transitions, 2) EDOC law, and 3) improving the event-action map.

146

147   *3.1 Identification of critical state transitions for decision variables*

148   To find state variables' changes leading to an obvious variation of decision variables' optimal

149   values, it is necessary to first identify critical state transitions. These state variables should be

150   selected from weather data (such as outdoor temperature, humidity, solar radiation intensity),

151   operating states of the air-conditioning system (such as the on/off status of components), and/or

152   occupancy conditions. Then, analyze the impact of their variations on selected decision variables.

153

154   To this end, time-driven optimal control of AC systems is conducted over a period (from $t = 0$

155   to $t = l$). The matrix of the state transitions M_s and the matrix of the variation of the decision

156   variables' optimal values and M_v, as shown in Eqn. (3) and (4), are obtained from operating

157   data.

$$M_s = \begin{bmatrix} \Delta s_{1,1}^* & \Delta s_{1,2}^* & \cdots & \Delta s_{1,l}^* \\ \Delta s_{2,1}^* & \Delta s_{2,2}^* & \cdots & \Delta s_{2,l}^* \\ \vdots & \vdots & \ddots & \vdots \\ \Delta s_{m,1}^* & \Delta s_{m,2}^* & \cdots & \Delta s_{m,l}^* \end{bmatrix} \text{ with } \Delta s_{j,t}^* = \frac{s_{j,t}-s_{j,t-1}}{\max\limits_{t=1\to l}|s_{j,t}-s_{j,t-1}|}, \; j=1,\cdots,m, \; t=1,\cdots,l \quad (3)$$

$$M_v = \begin{bmatrix} \Delta v_{1,1}^{opt*} & \Delta v_{1,2}^{opt*} & \cdots & \Delta v_{1,l}^{opt*} \\ \Delta v_{2,1}^{opt*} & \Delta v_{2,2}^{opt*} & \cdots & \Delta v_{2,l}^{opt*} \\ \vdots & \vdots & \ddots & \vdots \\ \Delta v_{n,1}^{opt*} & \Delta v_{n,2}^{opt*} & \cdots & \Delta v_{n,l}^{opt*} \end{bmatrix} \text{ with } \Delta v_{i,t}^* = \frac{v_{i,t}^{opt}-v_{i,t-1}^{opt}}{\max\limits_{t=1\to l}|v_{i,t}^{opt}-v_{i,t-1}^{opt}|}, \; i=1,\cdots,n, \; t=1,\cdots,l \quad (4)$$

where $s_{j,t}$ is the value of the jth state variable at time t, and $v_{i,t}^{opt}$ is the optimal value of the ith decision variable at time t.

Then, the impact of state transitions on variations of decision variables' optimal values are investigated based on the obtained M_s and M_v. Available tools with respect to the identification of critical variables include sensitivity analysis (Saltelli et al. 2004; Tian 2013), feature selection (Guyon and Elisseeff 2003; Zhang and Wen. 2019), and mutual information (May et al. 2008; Kapetanakis, Mangina, and Finn 2017). Due to its simple and low computation cost, the regression-based sensitivity analysis is adopted in this study, which fits a linear regression to the model outputs and uses the regression coefficients as direct measures of sensitivity, as illustrated in studies by Saltelli et al. 2004. The state transitions corresponding to the coefficients with high magnitude are regarded as the critical ones. More details are given in Section 4.3. It is assumed that there are m_i critical transitions are identified for the ith decision variable v_i, denoted as $(\Delta s_1^i, \cdots, \Delta s_{m_i}^i)$, and $\bar{m}$ critical transitions in total for all decision variables. The map is obtained from the variable selection to link the decision variable and its critical state transitions as shown in Fig. 2.
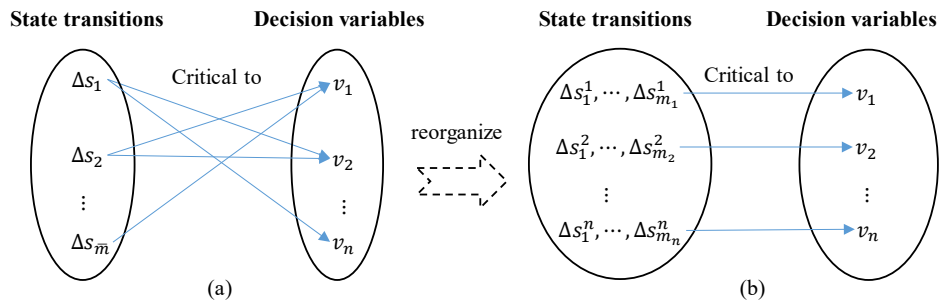

(a)   (b)

Fig. 2. (a) An initial map to show critical state transitions for decision variables (an example); (b) the improved map to link decision variables and their critical state transitions

3.2 EDOC law

To develop the event-driven paradigm, the important tasks are to build an event/action space, which contains all the events/actions, and a map to link the event and action space all together. The map specifies the appropriate action that should take place when an event occurs. To this end, the mathematical relationship between the variation of each decision variable's optimal value and its critical state transitions should be developed. Regression (Aranda et al. 2012), artificial neural network (ANN) (Kalogirou 2000), and support vector machine (SVM) (Jung, Kim, and Heo 2015) are most techniques commonly used for developing relationship in building energy systems. A simple and explicit regression mode is highly recommended for this study since the event occurrence should be calculated and identified timely. Besides, the relationship developed for event definition is only used to trigger the optimization, not to predict the optimal value of decision variables which are obtained through detailed system models after the trigger. Thus, a simple and explicit regression model can make the immediate identification and satisfy accuracy requirement with less striction.

The mathematical relationship between the critical state transitions and the decision variables is written as

$$\Delta v_i^{opt} = f^i(\Delta s_1^i, \cdots, \Delta s_{m_i}^i) \tag{5}$$

where f^i is a suitable mathematical function, which should be selected according to the data generated by a time-driven optimal control.

Assuming that the optimization of the decision variable v_i $(i = 1, \cdots, n)$ is necessary when the absolution value of Δv_i^{opt} is larger than a predefined threshold γ_i, then an event to trigger the optimization of v_i should be defined as

$$e^i: \left|f^i(\Delta s_1^i, \cdots, \Delta s_{m_2}^i)\right| > \gamma_i \tag{6}$$

Therefore, the event-driven optimal control (EDOC) law can be written as:

EDOC law: the decision variable $v_i, i \in [1, \cdots, n]$ should be optimized at time t if its critical states transition $(\Delta s_{1,t}^i, \cdots, \Delta s_{m_i,t}^i)$ satisfies $\left|f^i(\Delta s_{1,t}^i, \cdots, \Delta s_{m_2,t}^i)\right| > \gamma_i$.

The EDOC law defines the event and action spaces as well as the map between them, as shown in Fig. 3. There are n events and n actions, and each single event triggers one single action.

212 It should be noted that the threshold γ_i in this EDOC law is an important factor to balance the

213 optimization performance and the computational load. Its value should be specified by

214 considering multiple aspects including mainly the sensitivity of the energy consumption of the

215 AC system to the variation of decision variables, the control precision of control loops for

216 decision variables, and the fluctuation of the system operating state caused by the reset of
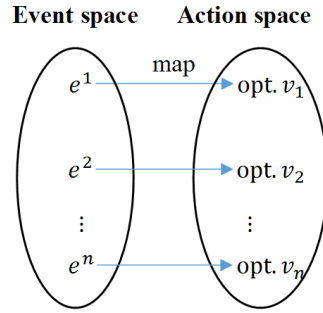
217 decision variables.

218

Event space   **Action space**

219 **Fig. 3**. Event and action space with the map directly from the EDOC law

220

221 *3.3 Improve the event-action map*

222 Fig. 3 indicates that when e_i occurs, only v_i needs to be optimized. However, in an

223 optimization problem, the global optimal solution can usually be achieved when all decision

224 variables are optimized simultaneously. This is due to the interaction between decision

225 variables which means the optimization of a variable is affected by values taken by other

226 variables (Li et al. 2016). Thus, if only the single corresponding decision variable is optimized

227 when an event occurs, the overall performance of the EDOC may be deteriorated. However, if

228 all decision variables are optimized simultaneously when any event occurs, the computation

229 load will increase considerably.

230

231 This problem can be avoided by analyzing the correlation among $\Delta v_i^{opt}, i = 1, \cdots, n$, and

232 merging the optimization actions of those decision variables with a high correlation coefficient.

233 The merging process is shown in Figure (4a), where Δv_i and Δv_j are assumed to be highly

234 correlated. In this case, v_j should be optimized when v_i is optimized and vice versa. Thus,

235 the optimization of v_i and v_j should be merged, *i.e.* whenever e^i or e^j occurs both v_i

236 and v_j should be optimized. When the optimization of highly correlated decision variables is

237 merged, the next step is to analyze the independence of the corresponding events and merge

238 events as necessary. For example, if the occurrence of e^i will lead to the occurrence of e^j,

239 then e^i and e^j can be merged as e^i. Note that this merging will not change the definition of

240 e^i as shown in Eqn. (6). The final event-action map is shown in Figure (3b), where the links

241 are categorized into two types: Type I where a single event will trigger the optimization of a

242 single decision variable; while in Type II a single event will trigger the optimization of multiple
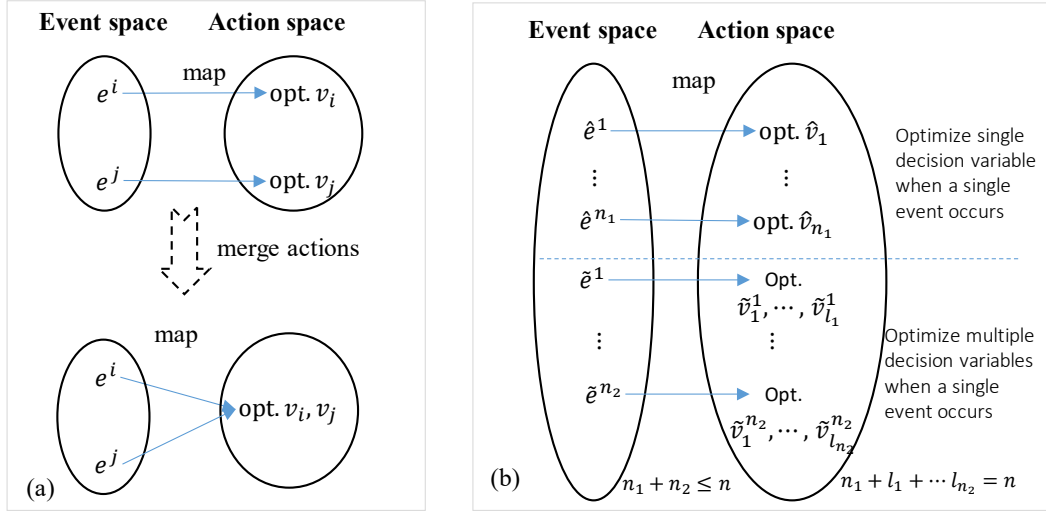
243 decision variables.

244

245

246

247 **Fig. 4**. (a) The process of merging actions; (b) improved map after the analysis of interaction

248 between decision variables

249

250 *3.4 Realization of the EDOC strategy*

251 After the event and action spaces, together with their map are established, EDOC can be

252 realized using the flowchart shown in Fig. 5. At each sampling time, all the critical state

253 transitions $(\Delta s_1, \cdots, \Delta s_{\bar{m}})$ need to be calculated, and hence the corresponding states $(s_1, \cdots, s_{\bar{m}})$

254 need to be monitored and their values at each sampling must be recorded. According to the

255 definitions of the events in the event space, the occurrence of each event should be detected. If

256 no event occurs, no optimization should be carried out at this time and therefore the values of

257 the all the decision variables should be maintained unchanged. Otherwise, there is a need to

258 find all the decision variables that should be optimized following the map between the event

259 space and the action space. Next, these variables are optimized using the adopted optimization
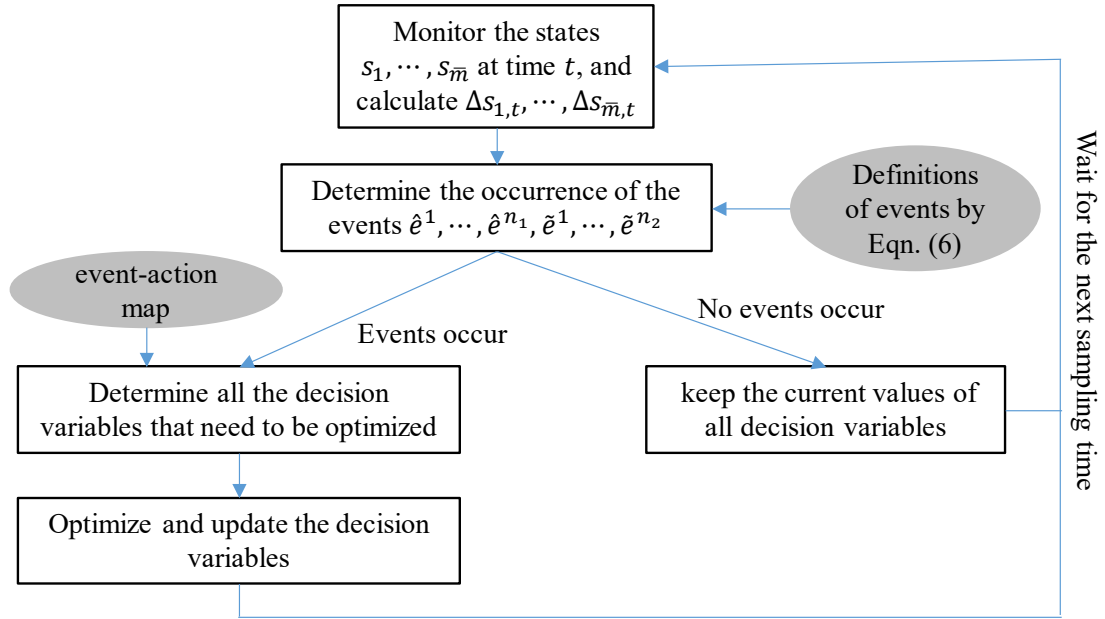
260 algorithm and updated to the new optimal values.

261

Fig. 5. Visualisation of the developed EDOC strategy

262
263

4. Case studies

In this section, the proposed mechanism to develop an EDOC strategy is illustrated through relevant case studies. A typical AC system was first selected, and then its simulation platform was established using TRNSYS and MATLAB. Based on this platform, operating data of AC systems were generated to develop and evaluate the EDO control strategy using the proposed method. The identification of critical state transitions and the establishment of an event-action map are explained below in detail.

4.1 Simulation platform

The selected typical air-conditioning system is illustrated in Fig. 6, which has three basic loops: the cooling water (CW), the chilled water (CHW), and the supply air (SA) loops. In the chilled water loop, the chiller is used to generate chilled water, which is delivered by a constant speed pump in the primary side and a variable speed (vs) pump in the secondary side. In the cooling water loop, a constant speed pump is used to cycle the cooling water, which dissipated heat to the ambient. In the supply air loop, the supply air is conditioned by an air-handling unit (AHU) and delivered to zones for cooling. During the operation, the CWS, CHWS, and the SA temperatures were under feedback control to track their preset set-points. The CWS, CHWS and SA temperatures were controlled by adjusting the cooling tower fan frequency, the flow rate of the refrigerant inside the chiller, and the flow rate of the chilled water through the AHU respectively.
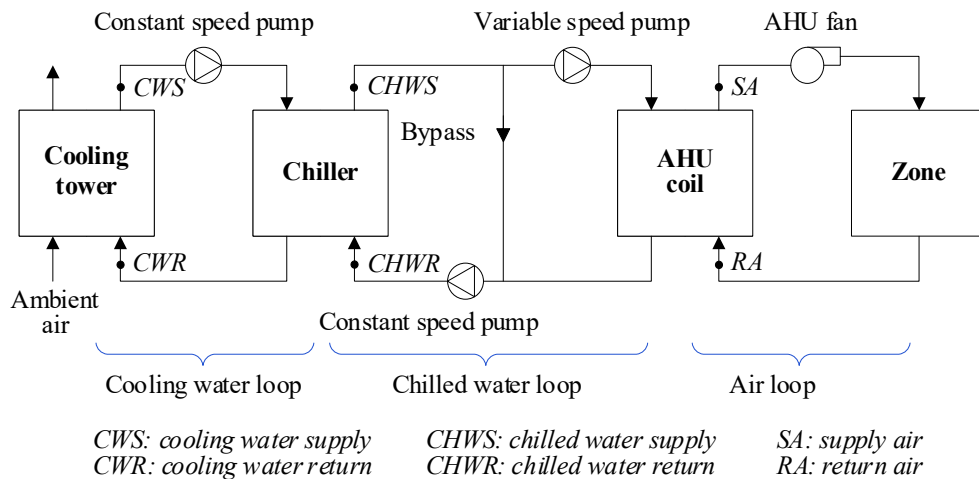
CWS: cooling water supply   CHWS: chilled water supply   SA: supply air
CWR: cooling water return   CHWR: chilled water return   RA: return air

Fig. 6. Schematic of a typical air-conditioning system

TRNSYS was chosen to establish the simulation platform for the AC system because of its proven capability to simulate the dynamics of AC systems. The type numbers of adopted components in TRNSYS and their parameter settings are presented in Table 1. All the component models used in this study are quasi-steady models. Note that external feedback controllers are not used for the control of the CHWS and the SA temperatures since Type 666 and Type 508c themselves assume that the set-points for the CHWS and the SA temperatures to be achieved respectively in their calculations. The performance data within Type 666 was rewritten according to the performance curve of a real chiller (Reform EIR Chiller Screw York YS 781kW/5.42COP/Valve) as described in the software DesignBuilder.

Table 1. Parameter settings of components in TRNSYS

Component	Parameter	Value
Chiller	Capacity (kW)	509
(Type 666)	COP	6.5
	Chilled water flow rate (kg/s)	23.6
	Cooling water flow rate (kg/s)	27.8
Cooling tower	Maximum air flow rate (m^3/s)	19.4
(Type 51b)	Rated power (kW)	5.5
	Cooling water flow rate (kg/s)	27.8
	Cooling capacity (kW)	604
CHW cs pump	Water flowrate (kg/s)	23.6
(Type 114)	Head (m)	15
	Rated power (kW)	5.1
CW cs pump	Water flowrate (kg/s)	27.8
(Type 114)	Head (m)	15
	Rated power (kW)	6
CHW vs pump	Water flowrate (kg/s)	23.6
(Type 110)	Head (m)	30
	Rated power (kW)	10.4
Coil (Type 508c)	Coil bypass fraction	0.15
Fan (Type 111b)	Rated air flow rate (kg/s)	37.3
	Rated power (kW)	40
CW PI controller	Gain constant	-0.1
(Type 23)	Integral time (hr)	0.2

Hong Kong weather for 2003 was selected as the operating environment of the AC system taken from the Hong Kong Observatory. The measured load profiles from a commercial building was used in the simulation. This commercial building had three cooling seasons:

303 spring, summer, and autumn as was recorded by the building energy management system
304 (BEMS),. The weather and load data of six days of each season; spring (April), summer
305 (August), and autumn (October) were used as the training condition to develop the event-driven
306 optimal control strategy (see below Section 4.3). The data of a day of each season; spring
307 (April), summer (August), and autumn (October) were used as the test condition to evaluate
308 the developed strategy, and the results are presented in Section 5. Basic information on weather
309 and load data is shown in Table 2.

310

311 **Table 2.** Weather and load condition

Item		Strategy development			Strategy evaluation		
		Spring	Summer	Autumn	Spring	Summer	Autumn
Db temp.	Max.	22.5	32.0	28.3	22.5	30.7	27.3
(°C)	Min.	18.4	25.9	21.6	19.8	26.9	22.1
	Mean	19.8	28.8	24.7	21.1	28.8	24.6
Wb temp.	Max.	21.5	27.7	22.6	21.5	27.5	19.7
(°C)	Min.	16.9	24.6	14.7	18.8	25.1	16.2
	Mean	18.9	26.5	18.8	20.3	26.2	17.8
Cooling load	Max.	216	462	344	216	446	294
(kW)	Min.	88	94	93	95	105	95
	Mean	135	264	198	161	290	203

312

313 *4.2 Formulation of real-time optimal control*

314 Due to no energy storage involved, the real-time optimal control was used to do the static
315 minimization of instantaneous power consumption of the whole system with respect to decision
316 variables at single time point (ASHRAE 2015). The objective function is given by Eqn. (7) and
317 the decision variables were these three set-points for the CWS, CHWS and SA temperature
318 controls.

319 $$P_{tot} = P_{ch} + P_{ct} + P_{chw,cs} + P_{chw,vs} + P_{cw,cs} + P_{fan} \qquad (7)$$

320 where P_{tot} is the instantaneous power of the total system; while P_{ch}, P_{ct}, $P_{chw,cs}$, $P_{chw,vs}$,
321 $P_{cw,cs}$, and P_{fan} are the power of the chiller, cooling tower, constant speed pump for chilled
322 water, variable speed pump for the chilled water, and constant speed pump for the cooling
323 water, and the fan of AHU respectively. The real-time optimization is then formulated as shown
324 in Eqn. (8):

325 $$\left[T_{cw,st}^{opt}(t), T_{chw,st}^{opt}(t), T_{sa,st}^{opt}(t) \right] = \underset{T_{cw,st}, T_{chw,st}, T_{sa,st}}{\arg\min} P_{tot}(t) \qquad (8)$$

326   where $T_{cw,st}$, $T_{chw,st}$, and $T_{sa,st}$ denote the set-points for the CWS, CHWS and SA

327   temperature respectively; while $T_{cw,st}^{opt}$, $T_{chw,st}^{opt}$, and $T_{sa,st}^{opt}$ denote their optimal values.

328

329   The constraints of this optimization problem were shown in Eqns. (9)-(10). The inequalities in

330   Eqn. (9) indicated that the values of the three decision variables were constrained by lower and

331   upper operating boundaries. The inequalities in Eqn. (10) were used to prevent the system

332   instability from large set-point changes. The operating boundaries of three decision variables

333   are given below in Table 3.

334
$$\begin{cases} T_{cw,st}^{L} \leq T_{cw,st} \leq T_{cw,st}^{U} \\ T_{chw,st}^{L} \leq T_{chw,st} \leq T_{chw,st}^{U} \\ T_{sa,st}^{L} \leq T_{air,st} \leq T_{sa,st}^{U} \end{cases} \tag{9}$$

335
$$\begin{cases} |T_{cw,st}(t) - T_{cw,st}(t-1)| \leq \Delta T_{cw,lm} \\ |T_{chw,st}(t) - T_{chw,st}(t-1)| \leq \Delta T_{chw,lm} \\ |T_{sa,st}(t) - T_{cw,sa}(t-1)| \leq \Delta T_{sa,lm} \end{cases} \tag{10}$$

336   where $T_{cw,st}^{L}/T_{cw,st}^{U}$, $T_{chw,st}^{L}/T_{chw,st}^{U}$, and $T_{sa,st}^{L}/T_{sa,st}^{U}$ are the lower/upper boundaries of

337    $T_{cw,st}$, $T_{chw,st}$, and $T_{sa,st}$ respectively, and $\Delta T_{cw,lm}$, $\Delta T_{chw,lm}$, and $\Delta T_{sa,lm}$ are the

338   limitation of set-point changes of $T_{cw,st}$, $T_{chw,st}$, and $T_{sa,st}$ respectively.

339

340   **Table 3**. Operating boundaries of decision variables

Boundary	Value (°C)
$[T_{cw,st}^{L}, T_{cw,st}^{U}]$	$[T_{wb}+1.5, 35]$
$[T_{chw,st}^{L}, T_{chw,st}^{U}]$	$[4, 10]$
$[T_{sa,st}^{L}, T_{sa,st}^{U}]$	$[12, 16]$

341

342   To obtain the relationship between these three temperatures set-points and the total power,

343   performance models for all power-consuming components are required. Here it is assumed that

344   these temperature set-points are well tracked, and thus the relationships between the power and

345   these three temperatures can be used directly. For the chillers, the DOE2 model described in

346   the study by Hydeman and Gillespie 2002, was adopted to predict the power and the CHWS

347   temperature for a given evaporator cooling load and the CHWS temperature. For the cooling

348   towers, the simplified cooling tower model in the paper by Lebrun et al. 2004 was used, which

349   was able to predict the required air flow rate for a given CWS temperature and thus the power

of the fans used in the cooling tower. The performance model of the AHU coils was developed based on Type 508c in TRNSYS. The coil model was able to predict the required CHW flow rate and the outlet water temperature given the CHWS temperature, the SA temperature and humidity. The power of variable speed pumps/fans was described using a cubic polynomial of fluid flowrate. The power of constant speed pumps/fans was constant and was set at their rated power. All undetermined parameters of performance models were identified using the components operating data in TRNSYS to make these performance models consistent with the component in TRNSYS.

The optimization algorithm was programmed using MATLAB and connected with TRNSYS using Type 155, an interface provided in TRNSYS to link TRNSYS and MATLAB. At each optimization time, a comprehensive search was adopted to find the optimal solutions. In this method, the total power P_{tot} was calculated when the decision variables varied from their lower to the upper boundary at a step change of 0.1℃. Here the step change of 0.1℃ was selected as relatively accurate solutions could be obtained and be used for the comparison studies in Section 5. The combination of the decision variables that made P_{tot} the minimum was the optimal solution $[T_{cw,st}^{opt}, T_{chw,st}^{opt}, T_{sa,st}^{opt}]$. The optimal solution was then transferred to TRNSYS and used as the set-points for the control of the CWS, CHWS and SA temperature respectively.

It should be noted that the optimization formulation for a real chiller plant with multiple chillers, cooling towers and AHUs might be much more complex than the one described by Eq. (8), especially when discrete and continuous decision variables are incorporated (Dullinger, Struckl, and Kozek. 2018). However, since the proposed EDOC strategy aims to build a map between events and actions and use existing techniques to solve optimization problems, it can be applied to any chiller plants.

4.3 Development of the EDOC strategy

The TDOC for the AC system was carried out under the training condition (18 days) with three different frequencies: every 30, 60 and 120 min (Wang and Ma 2008). In each optimization action, three temperature set-points were optimized simultaneously. Note the constraints in Eq. (10) were not considered in this study so that the operating data could fully reflect the influence

382   of state transitions on the variation of the optimal value of decision variables. In this way,

383   operating data for 18 days were obtained.

384

385   *4.3.1 Identification of critical state transitions for decision variables*

386   Since the operation of a chiller plant is mainly affected by its external operating conditions,

387   which can be characterized by the ambient dry-bulb temperature T_{db}, the ambient wet-bulb

388   temperature T_{wb}, and the part-load ratio (PLR) of the chiller plant (ASHRAE 2015), they were

389   considered as the states that had a potentially impact on the optimization of the chiller plant.

390   Therefore, critical state transitions were identified from the variation of these three state

391   variables for the optimization of the three decision variables $T_{cw,st}$, $T_{chw,st}$, and $T_{sa,st}$.

392

393   As illustrated in the theory of sensitivity analysis (Saltelli et al. 2004), the linear regression

394   coefficients of the input and output of a system can be used to measure the importance of input

395   on the output variables. Therefore, taking the state transitions as the input and the variation of

396   decision variables' optimal values as the output, regression coefficients matrix C_r in Eqn. (11)

397   is used as the indicator to identify critical state transitions in this case study.

$$M_v = C_r \cdot M_s \tag{11}$$

398

399   Fitting Eqn. (11) with the operating data, the regression coefficient matrix C_r for the whole

400   year (overall of the three seasons) was obtained and shown in Eqn. (12).

$$
\begin{bmatrix} \Delta T_{cw,st}^{opt,*} \\ \Delta T_{chw,st}^{opt,*} \\ \Delta T_{sa,st}^{opt,*} \end{bmatrix} = \begin{bmatrix} -0.027 & \mathbf{0.932} & \mathbf{0.495} \\ 0.019 & 0.010 & \mathbf{-0.997} \\ 0.023 & 0.06 & \mathbf{-1.016} \end{bmatrix} \cdot \begin{bmatrix} \Delta T_{db}^{*} \\ \Delta T_{wb}^{*} \\ \Delta PLR^{*} \end{bmatrix} \tag{12}
$$

401

402   The coefficients with high magnitude in each row are in bold in the matrix, where the

403   magnitude being larger than 0.1 was considered "high" as an example, and their corresponding

404   state transitions were regarded as the critical ones. Other state transitions were then considered

405   insignificant and their impacts were ignored. Therefore, three findings from the four coefficient

406   matrixes are as follows:

407   (1) The change in the ambient dry-bulb temperature ΔT_{db} had a little impact on the variations

408   of all these three decision variables; however, the wet-bulb temperature ΔT_{wb} had a

409   significant impact on all these three decision variables.

410   (2) For the CWS temperature set-point $T_{cw,st}$, its critical state transitions were ΔT_{wb} and

411   ΔPLR.

412　(3) For the CHWS temperature set-point $T_{chw,st}$ and the SA temperature set-point $T_{sa,st}$,

413　　their critical state transition was ΔPLR only.

414　The map linking the decision variables and their critical state transitions are shown in Fig. 7.
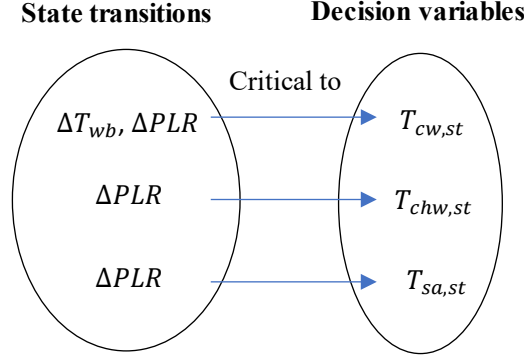

415

416　**Fig**. 7. The decision variable and its critical state transitions

417

418　*4.3.2 EDOC law*

419　The linear functions shown in Eqn. (13) were adopted to describe the relationship between the

420　variation of the decision variable optimal values and their critical state transitions:

421
$$
\begin{cases}
\Delta T_{cw,st}^{opt} = a_1 \cdot \Delta T_{wb} + b_1 \cdot \Delta PLR \\
\Delta T_{chw,st}^{opt} = b_2 \cdot \Delta PLR \\
\Delta T_{sa,st}^{opt} = b_3 \cdot \Delta PLR
\end{cases}
\tag{13}
$$

422　By fitting the operation data, into Eqn. (13) the linear models for the whole year were obtained

423　as presented in Eqn. (14), where the coefficient of determination (R^2) was also given. As can

424　be seen in Eqn. (14), R^2 of the linear was equal or greater than 0.9, which demonstrated that

425　the variations in the optimal values of the decision variables had a good linearity relationship

426　with their critical state transitions.

427
$$
\begin{cases}
\Delta T_{cw,st}^{opt} = 0.92 \cdot \Delta T_{wb} + 1.62 \cdot \Delta PLR & (R^2 = 0.92) \\
\Delta T_{chw,st}^{opt} = -6.71 \cdot \Delta PLR & (R^2 = 0.91) \\
\Delta T_{sa,st}^{opt} = -3.41 \cdot \Delta PLR & (R^2 = 0.90)
\end{cases}
\tag{14}
$$

428

429　To determine the threshold of the γ_i in Eqn. (6), the sensitivity of the total power to the

430　variations of the three set-points ($T_{cw,st}$, $T_{chw,st}$, $T_{sa,st}$) close to their optimal values was

431　analyzed. Using the simulation platform, the optimal values of these three set-points were

432　firstly calculated under multiple operating conditions where PLR was varied from 0.2 to 0.9

433　and T_{wb} from 18℃ to 27℃. The instantaneous power P of the AC system under these

multiple operating conditions was simulated with these three temperature set-points varying close to their optimal values. The results are summarized in Figure 8, where the horizontal axis δ_T indicate the deviation of the current temperature set-point T_{st} from its optimal value T_{st}^{opt} as shown in Eqn. (15); while the vertical axis $\delta_P\%$ is the change rate of the current instantaneous power P compared with the optimal instantaneous power P^{opt}, as shown in Eqn. (16).

$$\delta_T = T_{st} - T_{st}^{opt} \tag{15}$$

$$\delta_P\% = (P - P^{opt})/P^{opt} \tag{16}$$

It can be seen from Figure 8 that the instantaneous power close to the optimum was not very sensitive to the variations of these three temperatures. In detail, when the set-points deviated from the optimal values up to at least 0.4℃, the total instantaneous power was changed by 0.5% from the optimal value. The 'flat' optimum indicated that it was not necessary to optimize the system when any one of the three set-points deviated slightly from its optimal value (Braun 1989). Meanwhile, large values of δ_T should not be selected as the threshold for γ_i in Eqn. (6) because a large change in the set-points might cause the system to become unstable. In previous studies of the time-driven optimal control of the AC system [13, 32], set-point changes were usually constrained within 0.4 or 0.5℃. Therefore, considering the result of sensitivity study and the system stability, 0.4℃ was selected for all the three set-points. In this way, three events were defined as shown below in Eqn. (17). Thus, the event-action map was established as presented in Figure (9a).

$$\begin{cases} e^1: |0.92 \cdot \Delta T_{wb} + 1.62 \cdot \Delta PLR| \geq 0.4 \\ e^2: |6.27 \cdot \Delta PLR| \geq 0.4 \\ e^3: |3.23 \cdot \Delta PLR| \geq 0.4 \end{cases} \tag{17}$$
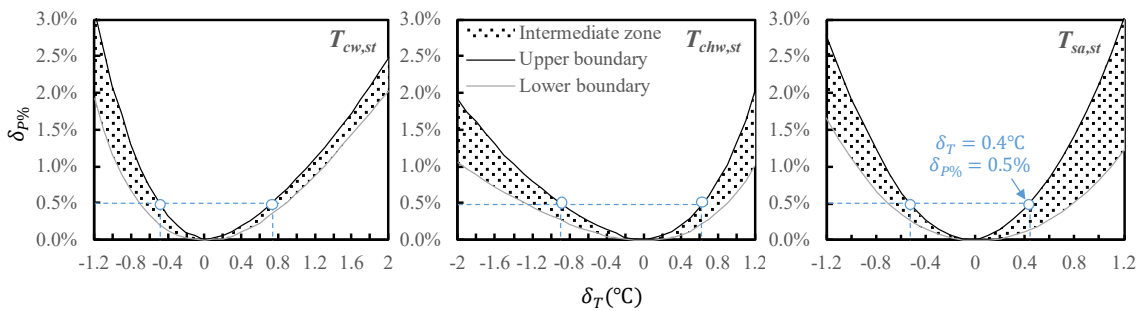

Fig. 8. Sensitivity of the instantaneous power of the AC system to the three temperatures near the optimal value

4.3.3 Improve the event-action map

To improve the event-action map, the interaction between decision variables were analyzed using simulation. To this end, four cases of the TDOC of the AC system were simulated, namely Base case, Case 1, Case 2, and Case 3, which are described in Table 4, where the fixed values are set according to the design guideline of ASHRAE Handbook (2015). In the base case, three decision variables are optimized simultaneously; while in other cases only two decision variables are optimized and the other is remained unchanged. A summer day was selected as an example for the detailed analysis.
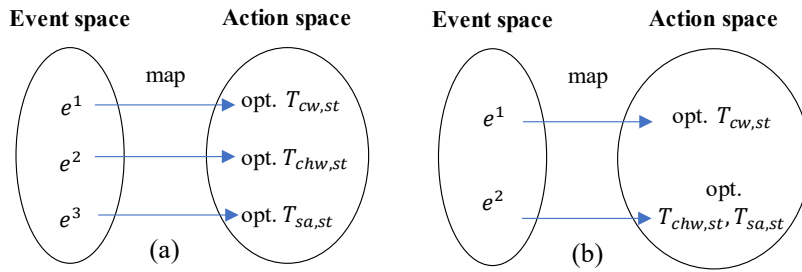

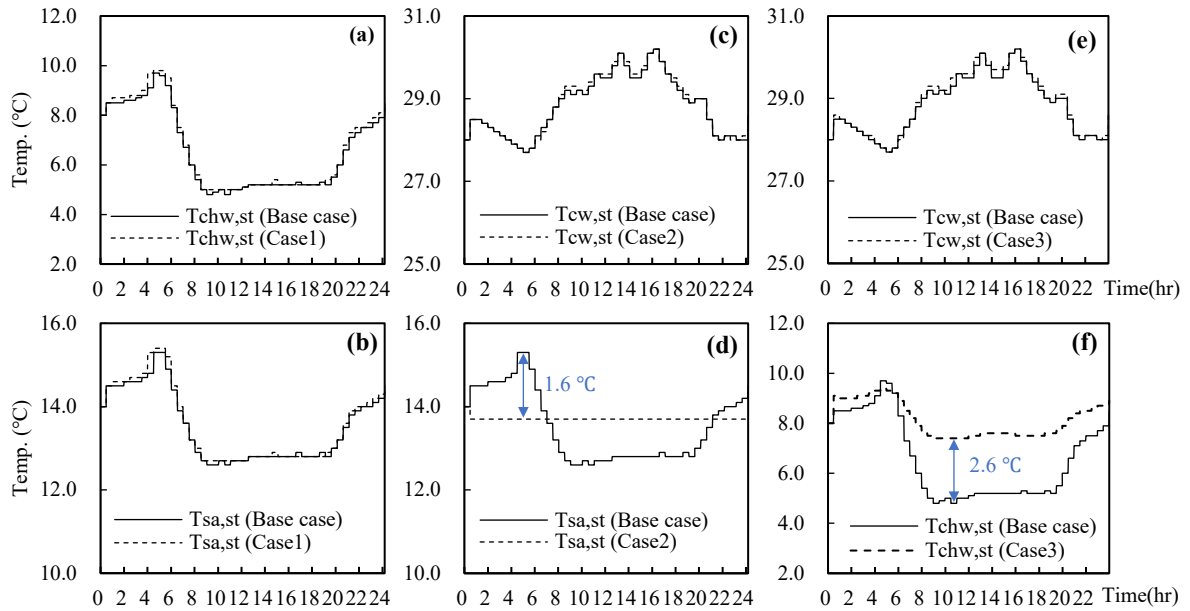**Fig. 9**. (a) The event-action map based on the EDOC law; (b) the improved map after merging events and actions

Fig. 10. Profiles of the three temperatures' optimal values for the research of decision variable interaction

477　　　　　　　　**Table 4**. Case information for the research of decision variable interaction

Case No.	Optimize	Fixed	Impact[*]
Base case	$T_{cw,st}, T_{chw,st}, T_{sa,st}$	-	-
Case 1	$T_{chw,st}, T_{sa,st}$	$T_{cw,st} = 30°C$	$T_{cw,st}$ on $T_{chw,st}, T_{sa,st}$
Case 2	$T_{cw,st}, T_{sa,st}$	$T_{chw,st} = 7°C$	$T_{chw,st}$ on $T_{cw,st}, T_{sa,st}$
Case 3	$T_{cw,st}, T_{chw,st}$	$T_{sa,st} = 15°C$	$T_{sa,st}$ on $T_{cw,st}, T_{chw,st}$

478　[*]: Because $T_{cw,st}$ in Case 1 was not optimized while it was optimized in the Base case, the comparison between

479　Case 1 and the Base case can help to observe the impact of the optimization of $T_{cw,st}$ on the optimization of

480　$T_{chw,st}$ and $T_{sa,st}$. If the optimal values of $T_{chw,st}$ and $T_{sa,st}$ in the Base case were consistent with those in Case

481　1, it can be concluded that the optimization of $T_{cw,st}$ had a little impact on the optimization $T_{chw,st}$ and $T_{sa,st}$.

482

483　The optimal values of the decision variables in the four cases are presented in Fig. 10. Fig. (10a)

484　and (10b) compared Case 1 (without optimization of T_{cw}) with the Based case, which showed

485　that the profiles of $T_{chw,st}^{opt}$ and $T_{sa,st}^{opt}$ in Case 1 were consistent with that in the Base case.

486　This indicated that the optimization of $T_{cw,st}$ might not significantly have an impact on the

487　optimization of $T_{chw,st}$ and $T_{sa,st}$. Fig. (10c) and (10d) compared Case 2 (without

488　optimization of $T_{chw,st}$) with the Base case, and Fig. (10e) and (10f) compared Case 3 (without

489　optimization of $T_{sa,st}$) with the Base case. Fig. (10c) and (10e) showed that the profiles of

490　$T_{cw,st}^{opt}$ in Case 2 and Case 3 were consistent with that in the Base case. It demonstrates that the

491　optimization of $T_{chw,st}$ and $T_{sa,st}$ might not have a significant impact on the optimization of

492　$T_{cw,st}$. Fig. (10d) and (10f) showed that $T_{sa,st}^{opt}$ in Case 2 and $T_{chw,st}^{opt}$ in Case 3 were largely

493　deviated from that in the Base case by up to 1.6 °C and 2.6 °C. This large deviation indicated

494　that $T_{chw,st}$ and $T_{sa,st}$ interact with each other, and thus the two temperatures should be

495　optimized simultaneously. In this way, the event-action map in Figure (9a) should be improved

496　as the one shown in Fig. (9b) by merging e^2 and e^3 as e^2.

497

498　*4.4 Optimal control algorithm*

499　Based on the determined event/action space and the event-action map, the algorithm of the

500　event-driven optimal control for the AC system was developed and its flowchart is shown in

501　Fig. 11. After starting the operation of the AC system, $T_{cw,st}$, $T_{chw,st}$ and $T_{sa,st}$ were

502　initially optimized to make sure that these three temperatures were optimal at the beginning

503　and the detection of the events could begin. Then, the ambient wet-bulb temperature T_{wb} and

504　the part-load ratio of the chiller PLR at each sampling period (e.g. every minute) were

505 monitored and recorded to detect the occurrence of the events e^1 and e^2. To guarantee the

506 operation stability, a time interval $\Delta\Gamma$ between two adjacent optimization actions for the same

507 decision variable should be greater than the time constant of the whole system. Due to the static

508 models adopted and immediate transient responses assumed in the simulation platform, 10-

509 minute was used here for minimum time interval for frequent optimization actions. When e^1

510 or e^2 was detected to occur and $\Delta\Gamma \geq 10\text{min}$, $T_{cw,st}$ or $T_{chw,st}$ and $T_{sa,st}$ should be

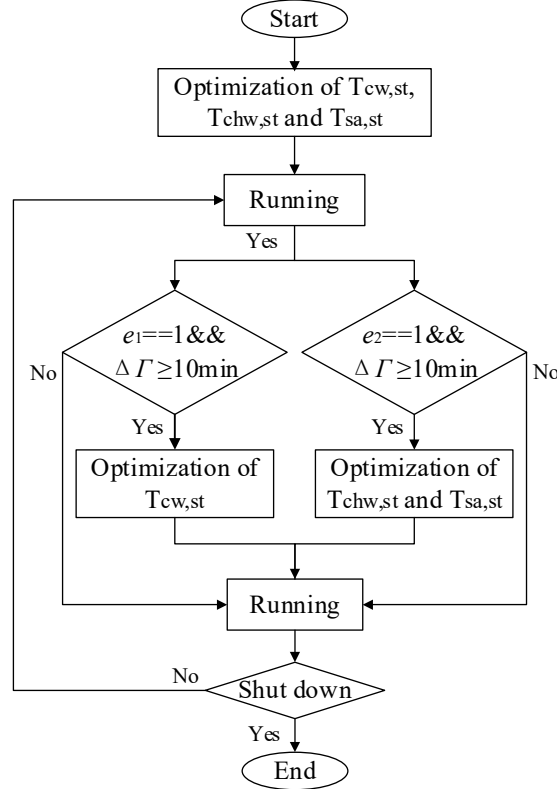511 optimized and their set-points updated accordingly.

512

513 **Fig. 11.** The flowchart of the event-driven optimal control for the AC system

514

515 **5. Results and Discussions**

516 To evaluate the developed EDOC algorithm, the operation of the AC system was simulated

517 under three strategies: operation without optimal control, operation with time-driven (every

518 30min) optimal control, and the developed strategy. In the operation without optimal control,

519 these three set-points were fixed at the specific values as listed in Table 5. In the operation with

520 time-driven and event-driven optimal control, the constraints in Eqn. (10) were considered

521 where values of $\Delta T_{cw,lm}$, $\Delta T_{chw,lm}$, and $\Delta T_{sa,lm}$ were $0.5°C$ to prevent a large change in set-

522 points. The operating environments included a spring, a summer, and an autumn day as shown

523 in Table 2.

Table 5. Fixed values of the three temperatures

Item	Spring (℃)	Summer (℃)	Autumn (℃)
$T_{cw,st}$	26	30	26
$T_{chw,st}$		7	
$T_{sa,st}$		15	

5.1 Optimization necessity

As previously mentioned, the development method of EDOC strategy presented in this study aims to achieve high necessity of optimization actions. To test whether it has been achieved, two evaluation indices are proposed, the action distance $d_{v_i,t}$ and average distance $\bar{d}$.

The action distance $d_{v_i,t}$ was used to evaluate the necessity of the single performed optimization action at time instant t for the decision variable v_i. As defined in Eqn. (18), it was the absolute variation of one decision variable's optimal value between two adjacent optimization actions. The larger the action distance, the higher the necessity of the action for v_i.

$$d_{v_i,t} = \left| v_{i,t}^{opt} - v_{i,t-1}^{opt} \right| = \left| \Delta v_{i,t}^{opt} \right| \tag{18}$$

where $v_{i,t}^{opt}$ is the ith decision variable's optimal value at time instant t.

The average distance $\bar{d}$ was used to evaluate the overall optimization necessity of an optimization strategy considering all performed optimization actions and all decision variables. It was calculated by Eqn. (19). The larger the index, the higher the overall optimization necessity is.

$$\bar{d} = \frac{\sum_{t=1}^{N_{opt}} \sum_{v_i=v_1}^{nv_t} \left| d_{v_i,t} \right|}{N_{opt}^{nv}} \tag{19}$$

where N_{opt}^{nv} is the weighted optimization times, N_{opt} is the number of optimization actions, nv_t is the number of optimized decision variables in the tth optimization action, N_{opt}^{nv} is the optimization times weighted by the number of the optimized decision variables in each optimization action and was calculated by the following equation:

$$N_{opt}^{nv} = \sum_{t=1}^{N_{opt}} nv_t \tag{20}$$

The action distance and average distance of TDOC and EDOC are calculated and presented in

551   Figure 12 and Table 6. Figure 12 gave the frequency distribution histogram of all action

552   distance in the two optimal control strategies. It can be observed that the action distances for

553   the three optimized temperatures in the TDOC were mainly inside the range of [0℃,0.1℃];

554   while most of action distances in the EDOC had a large value such as 0.4℃ or 0.5℃. The

555   average distance of the TDOC was 0.11℃ in spring, 0.15℃ in summer, and 0.14℃ in autumn;

556   while in the EDOC it was 0.39℃ in spring, 0.33℃ in summer, and 0.35℃ in autumn. The

557   large distance of the EDOC indicated that the defined events by the proposed development

558   method had effectively avoided unnecessary optimization actions and thus increased the overall

559   optimization necessity compared with the TDOC.

560

561   *5.2 Computation load*

562   The computation load of the two optimal control strategies was evaluated using the

563   computation time τ_{opt}. It refers to the time required by the optimization method to search for

564   optimal solutions. The computation time consumed by TDOC was 11.82s in spring, 11.18s

565   summer, and 11.92s and autumn as shown in Table 6. Compared with the TDOC, the relative

566   computation time saving r_{CS} was 83.9% in spring, 85.2% in summer, and 75.9% in autumn.

567   The great reduction in computation load in the EDOC strategy was caused by the removal of

568   unnecessary optimization actions and the decrease of the search dimension of the optimizations.

569   The search dimension of optimizations in EDOC control was decreased by the event-action

570   map. With the map, not all three temperatures were optimized in each optimization action, so

571   that the computation time for each optimization action was reduced. For example, the average

572   computation time for each optimization action and each temperature in the summer day was

573   τ_{opt}/N_{opt}^{nv} = 0.078s in the TDOC and 0.033s in the EDOC.

574

575   *5.3 Energy performance*

576   The energy performance of TDOC and EDOC strategies was compared with the operation

577   without optimization. As shown in Table 6, the daily energy consumption of the operation

578   without optimization was 976kWh in spring, 1747 kWh in summer and 1135 kWh in autumn.

579   The relative energy saving r_{ES} of TDOC was 4.4% in spring, 7.5% in summer, and 4.8% in

580   autumn, and that of the EDOC was 4.2% in spring, 7.4% in summer, and 4.8% in autumn

581   respectively. Therefore, the EDOC strategy achieved nearly the same energy performance as

582   that of the TDOC with a frequency of every 30 minutes. The reason for the effective energy

583   saving of the EDOC can be explained in Figure 13 and 14 when the summer day is taken as an

584   example. Figure 13 presents the operating conditions of the summer day, and Figure 14

585   compares the optimal values of the three set-points from the two optimal control strategies. It

586   is observed that the profiles of $T_{cw,st}^{opt}$, $T_{chw,st}^{opt}$ and $T_{sa,st}^{opt}$ in the two optimal control methods

587   were consistent. Besides, the EDOC responded more quickly to the rapid change of the

588   operation conditions. For example, the cooling load during 6:00 to 9:00 am increased rapidly

589   as shown in Figure 13. Figure (14b) and (14c) showed that optimization actions of the EDOC

590   were carried out more frequently and $T_{chw,st}^{opt}$ and $T_{sa,st}^{opt}$ changed more quickly than that in

591   the TDOC during the same period. In this way, energy saving effect of the EDOC strategy

592   developed by the proposed method can be guaranteed although weighted optimization times

593   are greatly reduced compared with the TDOC.

594   **Table 6.** Evaluation of event-driven optimization strategy

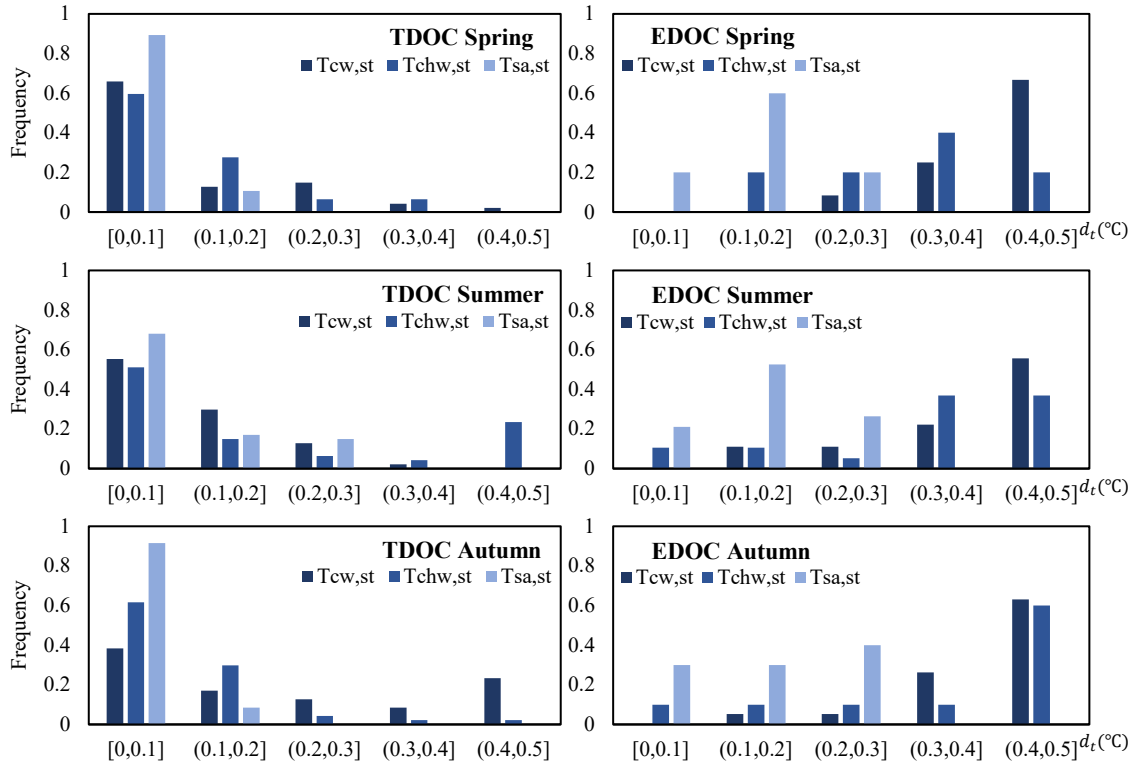| Case	Average distance (°C) $\overline{d}$	Opt. times N_{opt}^{nv}	Computation time (s) τ_{opt}	Computation saving r_{CS}	Energy (kWh) E_{ben} or E_{opt}	Energy saving r_{ES}
Spring						
No opt.	-	-	-	-	976	-
TDOC	0.11	144	11.82	-	933	4.4%
EDOC	0.39	27	1.90	83.9%	935	4.2%
Summer						
No opt.	-	-	-	-	1747	-
TDOC	0.15	144	11.18	-	1616	7.5%
EDOC	0.33	51	1.66	85.2%	1617	7.4%
Autumn						
No opt.	-	-	-	-	1135	-
TDOC	0.14	144	11.92	-	1080	4.8%
EDOC	0.35	42	2.87	75.9%	1081	4.8%

595

Fig. 12. Frequency distribution histograms of the optimization distance in TDOC and EDOC.
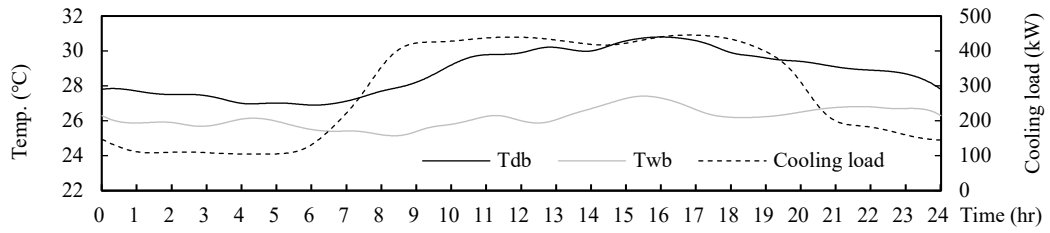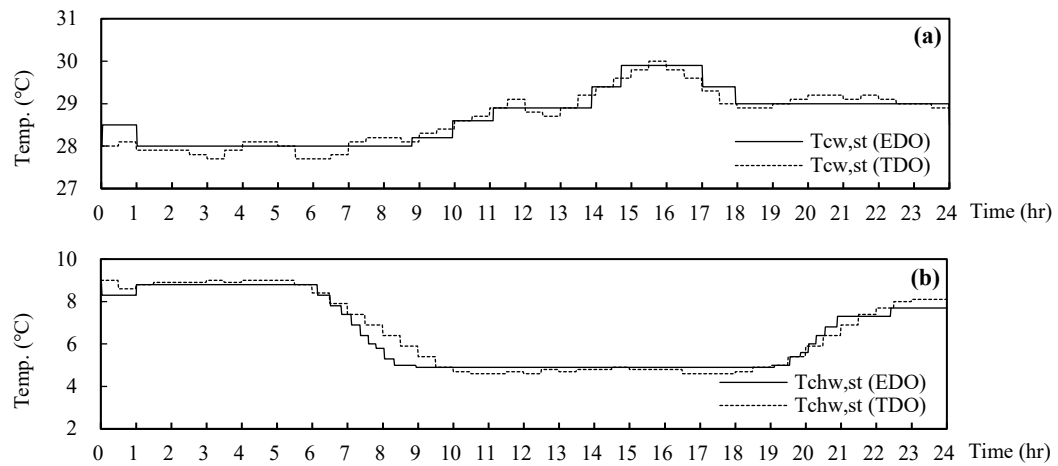

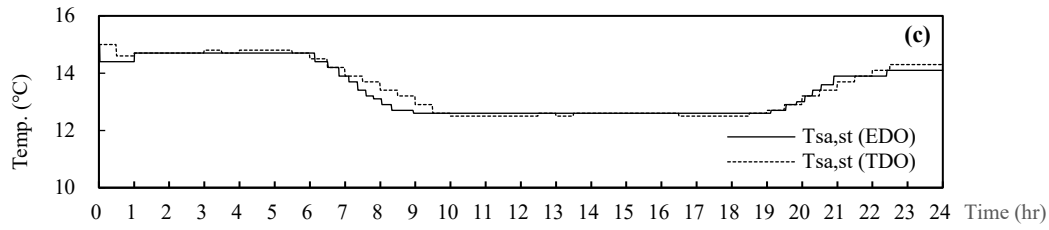**Fig. 13**. Profiles of operating conditions in the summer day

Fig. 14. Profiles of the three temperatures' optimal values in the summer day

6. Conclusions

This study has addressed the necessity of optimization actions in the real-time optimal control of air-conditioning systems, based on which a new method to develop event-driven optimal control is proposed. In the development method, the event/action space and the event-action map can be determined in a natural and systematic way, and not all the decision variables need to be optimized for a given event. The proposed method has been applied to a typical air-conditioning system, in which one event have been defined for the single optimization of a decision variable, the set-point for the cooling water supply temperature, and the other event for the combined optimization of other two decision variables including the set-points for the chilled water supply and the supply air temperatures. Compared with the operation with no optimization, the event-driven optimal control strategy can reduce 4.2-7.4% energy use, which is comparable to that of the time-driven optimal control (4.4-7.5%). Compared with the time-driven optimal control, the average distance in the event-driven optimization was 0.33-0.39℃, being 2.2-3.5 times of the time-driven control (0.11-0.15℃). Therefore, the developed event-driven optimization can achieve a significant computation load reduction up to 75.9-85.2% compared with the time-driven optimization (with a frequency of 30 mins) without scarifying the energy-saving potential.

In future work, the proposed method will be applied to a typical central air-conditioning system under different climates and for different types of buildings in order to identify generic events for air-conditioning systems. At the same time, the definition of events based on internal state transitions, such as on/off for major components, faults, and operators' intervention, will also be considered.

Reference

635 Aranda, A., G. Ferreira, M. Mainar-Toledo, S. Scarpellini, and E. L. Sastresa. 2012. "Multiple Regression Models
636   to Predict the Annual Energy Consumption in the Spanish Banking Sector." *Energy and Buildings* 49: 380-
637   387.

638 ASHRAE. 2015. ASHRAE Handbook - HVAC Applications (SI Edition). Atlanta, GA: ASHRAE.

639 Åström, K.J., and B. Bernhardsson. 1999. "Comparison of Periodic and Event based Sampling for First-order
640   Stochastic Systems." *IFAC Proceedings Volumes* 32: 5006-5011.

641 Borgers, D. P., V. S. Dolk, W. Heemels. 2017. "Riccati-based Design of Event-triggered Controllers for Linear
642   Systems with Delays." *IEEE Transactions on Automatic Control* 63: 174-188.

643 Braun, J. E., S.A. Clein, J. W. Mitchell, and W.A. Beckman. 1989. "Methodologies for Optimal Control of
644   Chilled-water Systems without Storage." *ASHRAE transactions* 95: 952-662.

645 Cao, X. R. 2008. "Stochastic Learning and Optimization - a Sensitivity-based Approach." *IFAC Proceedings
646   Volumes* 41: 3480-3492.

647 Cassandras, C.G. 2014. "The Event-driven Paradigm for Control, Communication and Optimization." *Journal of
648   Control and Decision* 1: 3-17.

649 Chang, Y.C., F.A. Lin, and C.H. Lin. 2005. "Optimal Chiller Sequencing by Branch and Bound Method for Saving
650   Energy." *Energy Conversion and Management* 46: 2158-2172.

651 Cumali, Z. 1988. "Global Optimization of HVAC System Operations in Real Time." *ASHRAE Transactions* 94:
652   1729-1744.

653 Dhar, N. K., N. K. Verma, and L. Behera. 2017. "Adaptive Critic-based Event-triggered Control for HVAC
654   System." *IEEE Transactions on Industrial Informatics* 14: 178-188.

655 Dullinger, C., W. Struckl, and M. Kozek. 2018. "A General Approach for Mixed-integer Predictive Control of
656   HVAC Systems Using MILP." *Applied Thermal Engineering* 128: 1646-1659.

657 Fisk, D.J. 2014. "Optimising Heating System Structure Using Exergy Branch and Bound." *Building Services
658   Engineering Research & Technology* 35: 321-333.

659 Guyon, I., and A. Elisseeff. 2003. "An Introduction to Variable and Feature Selection." *Journal of Machine
660   Learning Research* 3: 1157-1182.

661 Hydeman, M., and K. L. Gillespie. 2002. "Tools and Techniques to Calibrate Electric Chiller Component Models."
662   *ASHRAE transactions* 108: 733-741.

663 Jia, Q. S., J. Wu, Z. Wu, and X. Guan. 2018. "Event-based HVAC Control—A Complexity-based Approach."
664   *IEEE Transactions on Automation Science and Engineering* 15: 1909-1919.

665 Jung, H. C., J. S. Kim, and H. Heo. 2015. "Prediction of Building Energy Consumption using an Improved Real
666   Coded Genetic Algorithm based Least Squares Support Vector Machine Approach." *Energy and Buildings*
667   90: 76-84.

668 Kalogirou, S.A. 2000. "Applications of Artificial Neural-Networks for energy systems." *Applied energy* 67: 17-
669   35.

670 Kapetanakis, D. S., E. Mangina, and D. P. Finn. 2017. "Input Variable Selection for Thermal Load Predictive
671   Models of Commercial Buildings." *Energy and Buildings* 137: 13-26.

672 Kelman, A., Y. Ma, and F. Borrelli. 2013. "Analysis of Local Optima in Predictive Control for Energy Efficient
673   Buildings." *Journal of Building Performance Simulation* 6: 236-255.

674 Kusiak, A., M.Y. Li, and F. Tang. 2010. "Modeling and optimization of HVAC energy consumption." *Applied*
675   *Energy* 87: 3092-3102.

676 Lebrun, J., C.A. Silva, F. Trebilcock, and E. Winandy. 2004. "Simplified Models for Direct and Indirect Contact
677   Cooling Towers and Evaporative Condensers." *Building Services Engineering Research and Technology* 25:
678   25-31.

679 Li K., M. N. Omidvar, K. Deb, X. Yao. 2016. "Variable Interaction in Multi-objective Optimization Problems."
680   In: Handl J., Hart E., Lewis P., López-Ibáñez M., Ochoa G., Paechter B. (eds) Parallel Problem Solving from
681   Nature – PPSN XIV. PPSN 2016. Lecture Notes in Computer Science, vol. 9921. Springer, Cham.

682 Ma, Y., J. Matusko, and F. Borrelli. 2015. "Stochastic Model Predictive Control for Building HVAC Systems:
683   Complexity and Conservatism." *IEEE Trans. Contr. Sys. Techn.* 23: 101-116.

684 Ma, Z. J., and S. W. Wang. 2011. "Supervisory and Optimal Control of Central Chiller Plants using Simplified
685   Adaptive Models and Genetic Algorithm." *Applied Energy* 88: 198-211.

686 Martyr, R., J. Moriarty, and C. Beck. 2019. "Optimal Control of a Commercial Building's Thermostatic Load for
687   Off-peak Demand Response." *Journal of Building Performance Simulation* 12: 580–594.

688 May, R. J., H. R. Maier, G. C. Dandy, and T. G. Fernando. 2008. "Non-linear Variable Selection for Artificial
689   Neural Networks using Partial Mutual Information." *Environmental Modelling & Software* 23: 1312-1326.

690 Nassif N., S. Kajl, and R. Sabourin. 2005. "Optimization of HVAC Control System Strategy Using Two-objective
691   Genetic Algorithm." *HVAC&R Research* 11: 459-486.

692 Omidvar, M.N., X. Li, Y. Mei, and X. Yao. 2013. "Cooperative Co-evolution with Differential Grouping for Large
693   Scale Optimization." *IEEE Transactions on evolutionary computation* 18: 378-393.

694 Saltelli, A., S. Tarantola, F. Campolongo, and M. Ratto. 2004. "Sensitivity Analysis in Practice: A Guide to
695   Assessing Scientific Models." John Wiley & Sons Ltd, Chichester, West Sussex, England.

696 Shen, M., S. Yan, and G. Zhang. 2016. "A new Approach to Event-triggered Static Output Feedback Control of
697   Networked Control Systems." *ISA transactions* 65: 468-474.

698 Sun, Y. 2017. "On the Analysis of Interaction between Decision Variables." PhD thesis, Department of Mechanical
699   Engineering, the University of Melbourne.

700 Sun, Y.J., G.S. Huang, Z.W. Li, and S.W. Wang. 2013. "Multiplexed Optimization for Complex Air Conditioning
701   Systems." *Building and Environment* 65: 99-108.

702 Tian, W. 2013. "A Review of Sensitivity Analysis Methods in Building Energy Analysis." *Renewable and*
703   *sustainable energy reviews* 20: 411-419.

704 Waibel, C., G. Mavromatidis, R. Evins., and J. Carmeliet. 2019. "A Comparison of Building Energy Optimization
705   Problems and Mathematical Test Functions Using Static Fitness Landscape Analysis." *Journal of Building*
706   *Performance Simulation* 12: 789–811.

707 Wang, J., Q. S. Jia, G. S. Huang, and Y. J. Sun. 2018. "Event-driven Optimal Control of Central Air-conditioning
708   Systems: Event-space Establishment." *Science and Technology for the Built Environment* 24: 839-849.

709 Wang, J. Q., G. S. Huang, Y. J. Sun, and X. P. Liu. 2016. "Event-driven Optimization of Complex HVAC Systems."
710 *Energy and Buildings* 133: 79-87.

711 Wang, J. Q., P. Zhou, G. S. Huang, and W. Wang. 2017. "A Data Mining Approach to Discover Critical Events for
712 Event-Driven Optimization in Building Air Conditioning Systems." *Energy Procedia* 143: 251-257.

713 Wang, S. W. 2009. Intelligent Buildings and Building Automation. Spon Press, Taylor & Francis, London and
714 New York.

715 Wang, S. W., and Z. J. Ma. 2008. "Supervisory and Optimal Control of Building HVAC Systems: a Review."
716 HVAC&R Research 14: 3-32.

717 Wu, Z., Q. S. Jia, and X. Guan. 2015. "Optimal Control of Multi-room HVAC System: An Event-based Approach."
718 *IEEE Transactions on Control Systems Technology* 24: 662-669.

719 Xia, M., V. Gupta, and P.J. Antsaklis. 2016. "Networked State Estimation over a Shared Communication Medium."
720 *IEEE Transactions on Automatic Control* 62: 1729-1741.

721 Xu, Z., G. Hu, C. J. Spanos, and S. Schiavon. 2017. "PMV-based Event-triggered Mechanism for Building Energy
722 Management under Uncertainties." *Energy and Buildings* 152: 73-85.

723 Zhang, L., and J. Wen. 2019. "A Systematic Feature Selection Procedure for Short-term Data-driven Building
724 Energy Forecasting Model Development." *Energy and Buildings* 183: 428-442.

725 Zhu, F., M. Xia, and P. J. Antsaklis. 2014. "Passivity Analysis and Passivation of Interconnected Event-triggered
726 Feedback Systems using Passivity Indices." *IFAC Proceedings Volumes* 47: 11177-11182.

727